Draft version October 10, 2022
Typeset using LaTeX **twocolumn** style in AASTeX63

arXiv:2202.05618v3 [astro-ph.HE] 7 Oct 2022

Mergers of supermassive and intermediate-mass black holes in galactic nuclei from disruptions of star clusters

Giacomo Fragione[1,2]

[1] *Center for Interdisciplinary Exploration & Research in Astrophysics (CIERA) and Department of Physics & Astronomy, Northwestern University, Evanston, IL 60208, USA*

[2] *Department of Physics & Astronomy, Northwestern University, Evanston, IL 60202, USA*

ABSTRACT

Gravitational waves (GWs) offer an unprecedented opportunity to survey the sky and detect mergers of compact objects. While intermediate-mass black holes (IMBHs) have not been detected beyond any reasonable doubt with either dynamical or accretion signatures, the GW landscape appears very promising. Mergers of an IMBH with a supermassive black hole (SMBH) will be primary sources for the planned space-based mission LISA and could be observed up to the distant Universe. SMBH-IMBH binaries can be formed as a result of the migration and merger of stellar clusters at the center of galaxies, where an SMBH lurks. We build for the first time a semi-analytical framework to model this scenario, and find that the the comoving merger rate of SMBH-IMBH binaries is $\sim 10^{-4}$ Gpc^{-3} yr^{-1} in the local Universe for a unity IMBH occupation fraction, scales linearly with it, and has a peak at $z \approx 0.5$-2. Our model predicts ~ 0.1 event yr^{-1} within redshift $z \approx 3.5$ if 10% of the inspiralled star clusters hosted an IMBH, while ~ 1 events yr^{-1} for a unity occupation fraction. More than 90% of these systems will be detectable with LISA with a signal-to-noise ratio larger than 10, promising to potentially find a family of IMBHs.

1. INTRODUCTION

The formation and evolution of the innermost galactic regions is still uncertain. Most of the observed galactic nuclei harbour supermassive black holes (SMBHs), with masses $\sim 10^5$ - 10^9 (e.g., Ferrarese & Merritt 2000; Kormendy & Ho 2013). Galaxies across the entire Hubble sequence also show the presence of nucleated central regions, the nuclear star clusters (NSCs). NSCs are generally very massive, with mass up to a few times 10^7 $M_\odot$, and very dense, with half-light radius of a few pc (e.g., Georgiev et al. 2016; Neumayer et al. 2020). In some galaxies, as our own Milky Way, SMBHs and NSCs are found to co-exist (e.g., Capuzzo-Dolcetta & Tosta e Melo 2017).

NSCs typically contain a predominant old stellar population, with age $\gtrsim 1$ Gyr, and show also the presence of a young stellar population, with age $\lesssim 100$ Myr (e.g., Böker et al. 2001; Rossa et al. 2006; Carson et al. 2015; Minniti et al. 2016; Kacharov et al. 2018). While the latter requires some local recent star formation event, the former is comprised of stars as old as globular clusters (GCs). Therefore, a natural way to explain the origin of this population is through GC migration, and subsequent disruption, to the galactic center due to dynamical friction (e.g., Tremaine et al. 1975; Capuzzo-Dolcetta & Miocchi 2008; Antonini et al. 2012; Antonini 2013; Gnedin et al. 2014).

GCs represent a promising environment for forming intermediate-mass black holes (IMBHs), with masses in the range $\sim$ 10^2 - 10^4 $M_\odot$. This would also be expected assuming that the observed relation between the SMBH mass and the velocity dispersion of stars around it holds at lower masses (e.g., Ferrarese & Merritt 2000; Tremaine et al. 2002). A number of studies has shown that a likely venue to form an IMBH is the so-called runaway scenario, in the early phases of cluster evolution. In this process, the most massive stars segregate and merge in the core of the cluster, forming a massive growing object that could later collapse to form an IMBH (e.g., Portegies Zwart & McMillan 2002; Gürkan et al. 2004; Freitag et al. 2006; Giersz et al. 2015; Kremer et al. 2020; Di Carlo et al. 2021; González et al. 2021).

If an IMBH were to lurk in GCs that contribute to the assembly of NSCs, IMBHs would naturally be delivered to galactic nuclei in the proximity of an SMBH (e.g., Gürkan & Rasio 2005; Mastrobuono-Battisti et al. 2014; Arca-Sedda & Gualandris 2018; Fragione et al. 2018a,b; Arca-Sedda & Capuzzo-Dolcetta 2019; Askar et al. 2021). The evolution of the SMBH-IMBH binary may depend on the specific orbit of the parent GC, on the details of the local stellar density profile, and on the number of IMBHs that are simulataneously delivered (Baumgardt et al. 2006; Portegies Zwart et al. 2006; Mastrobuono-Battisti et al. 2014; Dosopoulou & An-

giacomo.fragione@northwestern.edu

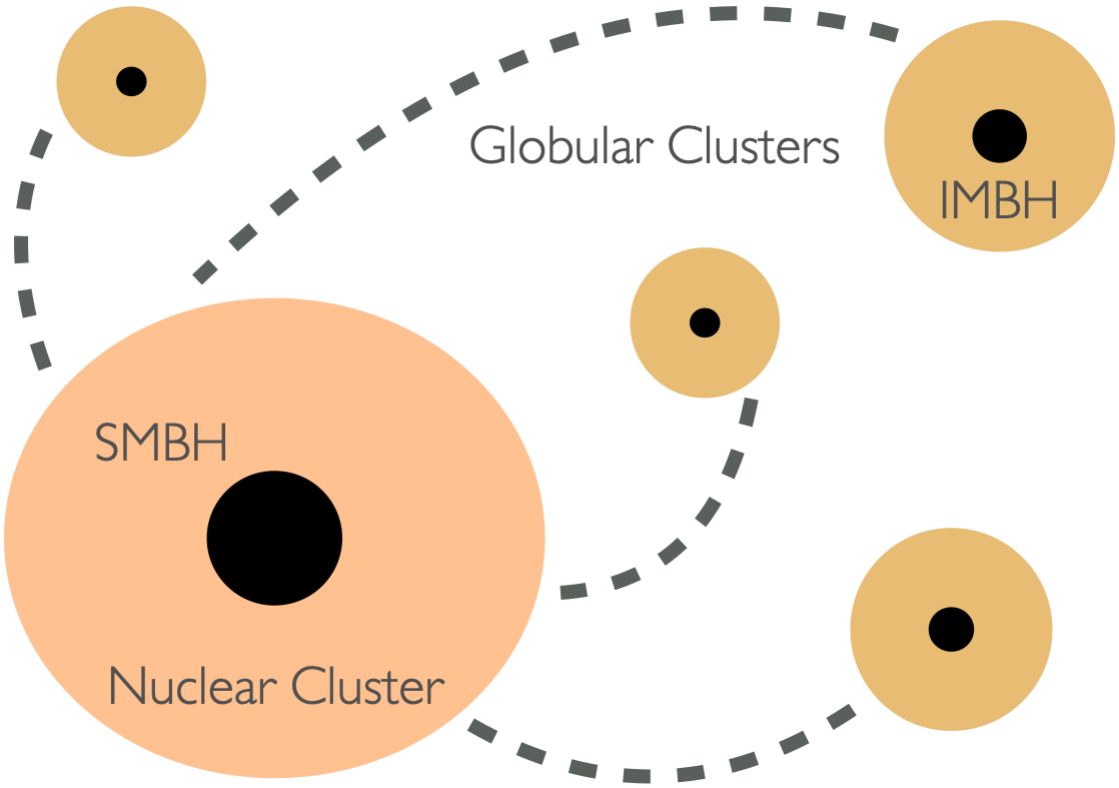


Figure 1. Schematic illustration of the formation of an NSC as a result of GC migration and disruption due to dynamical friction. An SMBH sits in the center of the NSC, while IMBHs are assumed to be in the center of infalling GCs. As a result of cluster disruption, an SMBH-IMBH binary is formed, which will eventually merge via GW emission and be detectable with LISA.

tonini 2017). Eventually, the binary merges via gravitational wave (GW) emission (see Figure 1 for a schematic illustration).

SMBH-IMBH mergers will be primary sources for LISA and could be observed up to the distant Universe (e.g., Amaro-Seoane et al. 2017; Jani et al. 2020). Despite their relevance, there have been only a handful attempts to model and compute the merger rate of SMBH-IMBH binaries resulting from migration and disruption of GCs in galactic nuclei (Arca-Sedda & Gualandris 2018; Arca-Sedda & Capuzzo-Dolcetta 2019). In this paper, we build for the first time a semi-analytical framework to model cluster disruptions and formation of SMBH-IMBH binaries, to compute their merger rates, and to assess their detectability with LISA. Our approach allows us to rapidly probe how the merger rates of SMBH-IMBH binaries are affected by galaxy masses, NSC and GC properties, and IMBH occupation fraction.

This paper is organized as follows. In Section 2, we discuss our numerical semi-analytical method to model SMBH-IMBH mergers. In Section 3, we present our results. Finally, in Section 4, we discuss the implications of our findings and draw our conclusions.

2. METHOD

In what follows, we describe the details of SIMBHME[1], the numerical method we use to follow the formation and evolution of SMBH-IMBH binaries.

We start with sampling galaxy masses $M_{*,\rm gal}$ from a Schechter function

$$\Phi(M_{*,\rm gal},z)=\Phi_*(z)\left(\frac{M_{*,\rm gal}}{M_{\rm c}(z)}\right)^{\alpha_{\rm c}(z)}\exp\left(-\frac{M_{*,\rm gal}}{M_{\rm c}(z)}\right), \quad (1)$$

from $M^{\rm min}_{*,\rm gal}=10^{8.5}\,M_\odot$ to $M^{\rm max}_{*,\rm gal}=10^{10.75}\,M_\odot$, corresponding approximately to the range where NSCs and SMBHs would co-exist (e.g., Capuzzo-Dolcetta & Tosta e Melo 2017). We set $\Phi_*(z=0)=0.8\times10^{-3}$ Mpc^{-3}, $M_{\rm c}(z=0)=10^{11.14}\,M_\odot$, and $\alpha_{\rm c}(z=0)=-1.43$, as extracted from the EAGLE cosmological simulations in Furlong et al. (2015), which are consistent with the observed distribution of galaxies. While the galaxy distribution evolves as a function of redshift, we sample galaxy masses using the present-day distribution. This

[1] https://github.com/giacomofragione/simbhme

procedure ensures that the statistical distributions of galaxy masses, NSC masses, and SMBH masses in our model are consistent with the respective observed distributions in the local Universe. We take into account the redshift dependence of Eq. 1 when computing the merger rates (see Eq. 8), where we reweigh the galaxy sample according to the galaxy distribution at a given redshift. For the evolution of the galaxy mass function as a function of redshift, see Table A1 in Furlong et al. (2015).

We use scaling relations from Georgiev et al. (2016) for galaxies that host both an NSC and an SMBH, and compute the sum of their masses from

$$\log((M_{\rm NSC}+M_{\rm SMBH})/\gamma_1) = \zeta\times\log(M_{*,\rm gal}/\gamma_2)+\psi\,, \quad (2)$$

where $\gamma_1 = 5.03\times10^7\,M_\odot$, $\gamma_2 = 2.76\times10^{10}\,M_\odot$, $\zeta = 1.491$, $\psi = -0.019$. Note that this relation does not depend on the galaxy type. In sampling from Eq. 2, we consider the scatter in the fit parameters. Then, to compute the SMBH and NSC masses, we fit data in Figure 7 of Georgiev et al. (2016) with

$$\log(M_{\rm SMBH}/M_{\rm NSC}) = A\times\log(M_{*,\rm gal}) + B\,. \quad (3)$$

From our least-square fit, we find $A = 2.05$ and $B = -20.92$, with dispersion $\sigma = 1.54$. Also in this case, we consider the scatter in the fit parameters when sampling from Eq. 3, and we discard from our analysis galaxies whose central SMBH or NSC would be less massive than $10^5\ M_\odot$.

We now compute the fraction of NSC mass formed as a consequence of GC migration and disruption, $f_{\rm out}$. We adopt the results of Fahrion et al. (2021), where a semi-analytical model of NSC formation based on the orbital evolution of inspiraling GCs, together with observed NSC and GC system properties, was used to estimate the NSC mass formed *in-situ* through local star formation. Following their approach, we first compute the mass formed *in-situ*

$$f_{\rm in} = \beta\tanh(\log(M_{\rm NSC}) - \alpha) + (1-\beta)\,, \quad (4)$$

where $\alpha = 7.28$ and $\beta = 0.34$ (dispersion $\sigma_{\rm in} = 0.12$). Then, we simply estimate the fraction of mass accreted from GC disruptions as $f_{\rm out} = 1 - f_{\rm in}$.

Individual GC masses are sampled from the GC initial mass function, which we assume to be described by a negative power-law (Gieles 2009; Larsen 2009; Chandar et al. 2010, e.g.,)

$$f(M_{\rm GC}) \propto M_{\rm GC}^{-2}\,, \quad (5)$$

from $M_{\rm GC,min} = 10^5\,M_\odot$ to $M_{\rm GC,max} = f_{\rm out}M_{\rm NSC}$. We sample GC masses until the total sampled mass is $M_{\rm out} = f_{\rm out}M_{\rm NSC}$, and draw cluster cosmic formation times from (e.g., Gratton et al. 1997, 2003; VandenBerg et al. 2013; El-Badry et al. 2019)

$$\psi(z) \propto \exp[-(z-z_{\rm GC})^2/\sigma_{\rm GC}]\,, \quad (6)$$

where $z = 3.2$ and $\sigma_{GC} = 1.5$[2].

In dense star clusters, IMBHs could be originated mainly through repeated mergers either of massive main-sequence stars, later collapsing to form an IMBH, (Portegies Zwart & McMillan 2002; Gürkan et al. 2004; Freitag et al. 2006; Pan et al. 2012; Giersz et al. 2015; Tagawa et al. 2020; Di Carlo et al. 2021), or of stellar-mass BHs (Miller & Hamilton 2002; O'Leary et al. 2006; Antonini & Rasio 2016; Antonini et al. 2019; Fragione et al. 2022; González et al. 2021; Mapelli et al. 2021; Weatherford et al. 2021). Both processes depend on a number of initial cluster properties, including its density, primordial binary fraction, and the slope of the initial mass function. The mass distribution and the occupation fraction (that is the fraction of clusters that form an IMBH) of IMBHs is quite uncertain. For simplicity, we take the IMBH masses to be a fixed fraction

$$\zeta = \frac{M_{\rm IMBH}}{M_{\rm GC}} \quad (7)$$

of the initial cluster mass. We consider different models with $\zeta = 0.001$, 0.003, 0.005, and we take the IMBH occupation fraction in GCs, $f_{\rm GC}^{\rm IMBH}$, to be 0.1, 0.3, 0.5, 1.0.

After the host GC delivers its central IMBH in the innermost regions of a galaxy, the formation, evolution, and eventual merger via GW emission of SMBH-IMBH binaries may depend on the specific orbit of the parent cluster, on the details of the local stellar density profile, and on the number of IMBHs that are simultaneously delivered (Baumgardt et al. 2006; Portegies Zwart et al. 2006; Mastrobuono-Battisti et al. 2014; Dosopoulou & Antonini 2017). For example, if the orbit of the parent cluster is not sufficiently elliptic, the emission of GWs could not be efficient in merging the SMBH-IMBH binary, or the interaction of IMBHs of $\sim 100\,M_\odot$ with the stars and compact objects surrounding the SMBH could quench the merger via GW emission (e.g., Arca Sedda et al. 2019; Arca-Sedda & Gualandris 2018). For simplicity, we assume that the delay time (from cluster formation to SMBH-IMBH merger) follows an exponential distribution with mean $\tau = 1$ Gyr (Arca-Sedda & Gualandris 2018). Note that this implies that the IMBH would have had enough time to be assembled between cluster formation and cluster disruption. This eventuality would be likely in the case the IMBH originates as a consequence of a rapid runaway process that could take place within ~ 10 Myr from the cluster birth, while it would be more challenging if the IMBH grows primarily as a result of repeated mergers of stellar-mass BHs (e.g., Giersz et al. 2015; González et al. 2021; Fragione et al. 2022). To check how our results depend on the

[2] We assume that the assembly of NSCs occurs within $\sim$ 10-100 Myr of the formation of GCs (e.g., Antonini et al. 2012; Antonini 2013; Gnedin et al. 2014).

assumed distribution of delay times, we also run models with a $1/t$ distribution and a uniform distribution, with $t_{\rm min} = 0.5\,{\rm Gyr}$ and $t_{\rm max} = 10\,{\rm Gyr}$ being the minimum and maximum delay time, respectively.

3. RESULTS

3.1. *Mass and mass-ratio distributions*

We show in Figure 2 the probability distribution functions of the mass of IMBHs in SMBH-IMBH binaries that merge within a Hubble time in our simulations for different assumption on the IMBH mass, taken to be a fraction ζ of its parent cluster mass. In these models, $f_{\rm GC}^{\rm IMBH} = 1.0$ and the delay time follows an exponential distribution with mean $\tau = 1\,{\rm Gyr}$. We find that about 50% of the IMBHs that merge with an SMBH within a Hubble time have masses $\lesssim 200\ M_\odot$, $\lesssim 400\ M_\odot$, $\lesssim 1000\ M_\odot$ for $\zeta = 0.001$, $\zeta = 0.003$, $\zeta = 0.005$, respectively. The slope of the distributions is independent of ζ and is $\propto M_{\rm IMBH}^{-2}$, as expected. Indeed, IMBH masses are scaled from GC masses, whose distribution is assumed to be $\propto M_{\rm GC}^{-2}$.

The bottom panel of Figure 2 shows the probability distribution functions of the mass ratio $q = M_{\rm IMBH}/M_{\rm SMBH}$ of SMBH-IMBH binaries that merge within a Hubble time as a function of ζ. We find that about 50% of the binaries have mass ratios $\lesssim 7\times10^{-5}$, $\lesssim 1\times10^{-4}$, 3×10^{-4} for $\zeta = 0.001$, $\zeta = 0.003$, $\zeta = 0.005$, respectively.

3.2. *Merger rates*

We compute the merger rates as

$$\Gamma(z) = \epsilon \frac{d}{dt} \int_{M_{*,\rm gal}^{\rm min}}^{M_{*,\rm gal}^{\rm max}} \frac{\partial N(z)}{\partial M_{*,\rm gal}} \Phi(z, M_{*,\rm gal}) dM_{*,\rm gal}\,, \quad (8)$$

where ϵ is the fraction of galaxies that host both an NSC and SMBH, and $\partial N(z)/\partial M_{*,\rm gal}$ is the number of mergers at a given redshift, z, per unit stellar galactic mass. The fraction of galaxies that host both an NSC and SMBH is highly uncertain and could depend on the galaxy mass and type (e.g., Neumayer et al. 2020). In our calculations, we assume an average value of $\epsilon = 0.3$[3], from the semi-analytical models of Antonini et al. (2015).

Figure 3 reports the comoving (top) and cumulative (bottom) merger rates for SMBH-IMBH binaries from cluster disruptions in galactic nuclei for different IMBH occupation fractions (solid lines). In these models, $\zeta = 0.001$ and the delay time follows an exponential distribution with mean $\tau = 1\,{\rm Gyr}$. We find that the comoving rate is $\sim 10^{-4}\ {\rm Gpc^{-3}\,yr^{-1}}$ in the local Universe for $f_{\rm GC}^{\rm IMBH} = 1.0$, has a peak at $z \approx 2$, and scales linearly with the IMBH occupation fraction. When considering the cumulative rate, we find that our model

[3] This value may evolve across cosmic time.

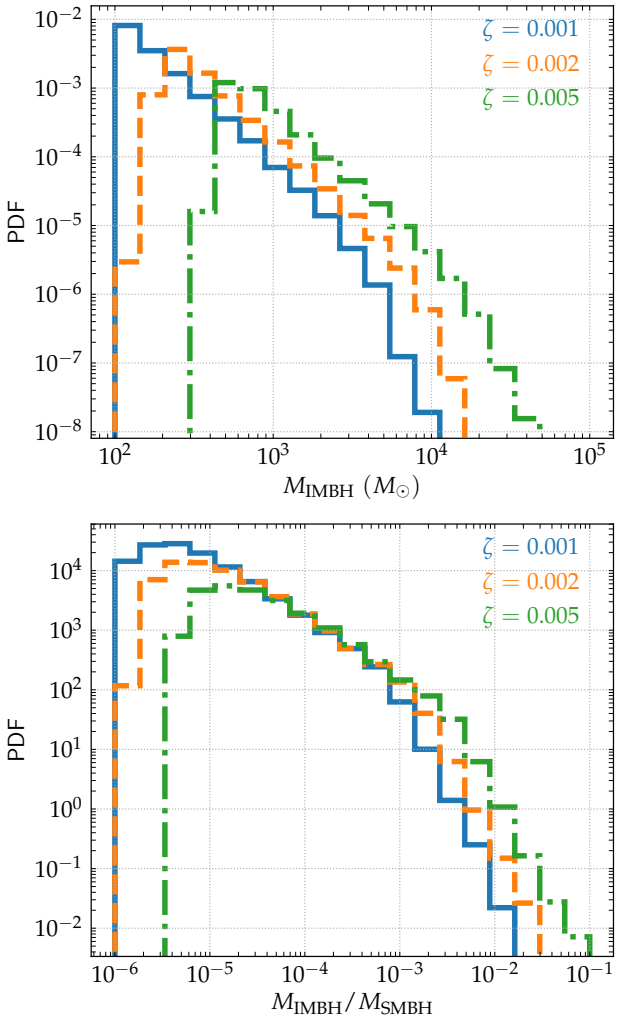


Figure 2. Probability distribution functions of the mass of IMBHs (top) and mass-ratio of SMBH-IMBH binaries (bottom) that merge within a Hubble time. Different colors represent different assumptions on the IMBH mass, taken to be a fraction ζ of the mass of its parent cluster. The occupation fraction is fixed to $f_{\rm GC}^{\rm IMBH} = 1.0$ and the delay time follows an exponential distribution with mean $\tau = 1\,{\rm Gyr}$.

predicts ~ 0.1 merger event ${\rm yr}^{-1}$ within redshift 3.5 if 10% of star clusters harbour an IMBH, while $\sim 1\ {\rm yr}^{-1}$ if every cluster were to host an IMBH. Note that our results are consistent with the order-of-magnitude estimates in Arca-Sedda & Gualandris (2018) and Arca-Sedda & Capuzzo-Dolcetta (2019), who used a combination of semi-analytical estimates and N-body models of a limited sample of infalling star clusters.

We also compute merger rates for a different choice of the minimum GC mass. Fahrion et al. (2021) argue that the minimum mass of GCs that inspiralled into the NSC scales $\propto R_{\rm eff}^2$, ($R_{\rm eff}$ is the effective radius of the galaxy) and can be approximately estimated by looking at the most massive cluster that has survived to present time.

We adopt the scaling relation between a galaxy size and its mass from Shen et al. (2003)

$$\log\left(\frac{R_{\rm eff}}{\rm kpc}\right) = \log b_1 + a_1 \log\left(\frac{M_*}{M_\odot}\right) \,, \qquad (9)$$

where $a_1 = 0.56$ and $b_1 = 3.47 \times 10^{-5}$, for early-type galaxies, and

$$\log\left(\frac{R_{\rm eff}}{\rm kpc}\right) = \log c_2 + a_2 \log\left(\frac{M_*}{M_\odot}\right) + (b_2 - a_2) \log\left(1 + \frac{M_*}{M_0}\right) \,, \qquad (10)$$

where $a_2 = 0.14$, $b_2 = 0.39$, $c_2 = 0.1$, $M_0 = 3.98 \times 10^{10}$ $M_\odot$, for late-type galaxies, and normalize to Milky Way's values, obtaining

$$M_{\rm GC,min} = 10^6 \; M_\odot \left(\frac{R_{\rm eff}}{4\,\rm kpc}\right)^2 . \qquad (11)$$

We report our results in Figure 3 (dotted line) for late-type galaxies, and find that comoving and cumulative merger rates decrease by a factor of about 2 with respect to case we assume $M_{\rm GC,min} = 10^5\ M_\odot$. Instead, in the case we consider early-type galaxies, the rates decrease by a factor of about 4.

In Figure 4, we report the comoving (top) and cumulative (bottom) merger rates for SMBH-IMBH binaries from cluster disruptions in galactic nuclei for different assumptions on delay times from cluster disruptions to SMBH-IMBH mergers both for $M_{\rm GC,min} = 10^5\ M_\odot$ (solid lines) and $M_{\rm GC,min}$ from Eq. 11 (dotted lines), assuming $f_{\rm GC}^{\rm IMBH} = 1.0$ and $\zeta = 0.001$. Rates for different values of the occupation fraction can be easily obtained by considering that rates scales linearly with $f_{\rm GC}^{\rm IMBH}$. We find that there is no significant difference in the total number of merger rates per year when we assume different distributions for delay times. However, while the comoving rate is peaked at $z \approx 2$ in the case of an exponential distribution, they are peaked at $z \approx 3$ for a $1/t$ distribution and at $z \approx 0.5$ for a uniform distribution, owing to typically shorter and longer delay times, respectively.

3.3. *LISA detections*

We now compute the signal-to-noise ratio (SNR) for an SMBH-IMBH binary merger in LISA band. Note that these binaries enter the LISA band and merge within the nominal mission lifetime (of about 5 yr).

We compute the average SNR as

$$\left\langle \frac{S}{N} \right\rangle = \frac{4}{\sqrt{5}} \sqrt{\int_{f_{\rm min}}^{f_{\rm max}} \frac{|\tilde{h}(f)|^2}{S_n(f)} df} \,, \qquad (12)$$

where $f_{\rm min}$ and $f_{\rm max}$ are the minimum and maximum frequency of the binary in the detector band, respectively, $S_n(f)$ is the effective noise power spectral density,

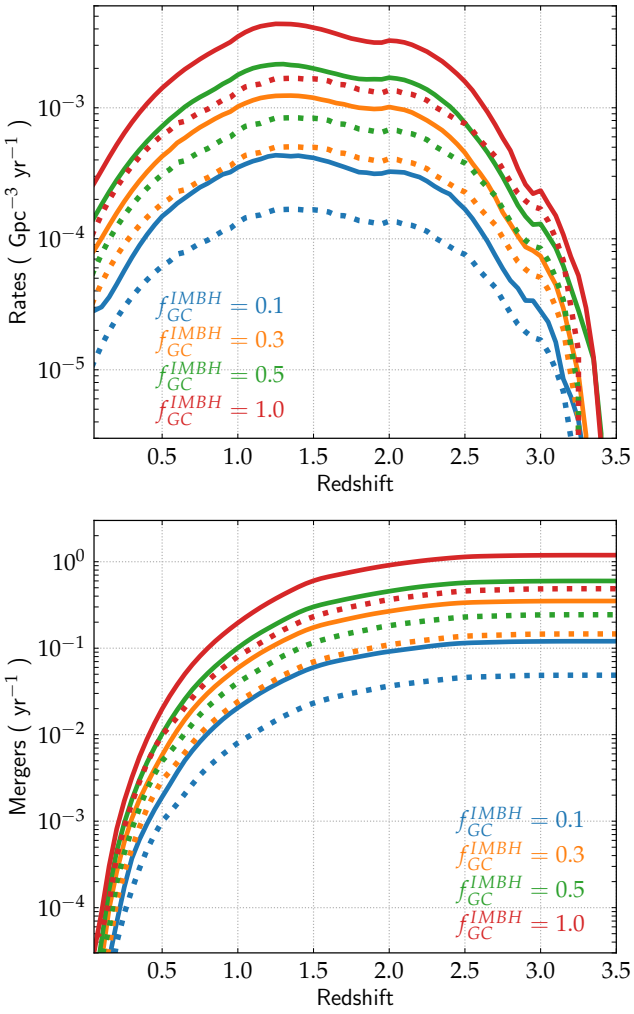


Figure 3. Comoving (top) and cumulative (bottom) merger rates for SMBH-IMBH binaries from cluster disruptions in galactic nuclei. In these models, $\zeta = 0.001$ and the delay time follows an exponential distribution with mean $\tau = 1$ Gyr. Different colors represent different IMBH occupation fractions. Solid lines: $M_{\rm GC,min} = 10^5\ M_\odot$; dotted lines: $M_{\rm GC,min}$ from Eq. 11 for late-type galaxies.

and $|\tilde{h}(f)|$ is the frequency-domain waveform amplitude, approximated with a PhenomA waveform (e.g., Eq. 20 in Robson et al. 2019)

$$|\tilde{h}(f)| = \sqrt{\frac{5}{24\pi^{4/3}}} \frac{G^{5/6}}{c^{3/2}} \frac{M_{\rm c,z}^{5/6}}{D_{\rm L} f_0^{7/6}} \times \begin{cases} (f/f_0)^{-7/6} & f < f_0 \\ (f/f_0)^{-2/3} & f_0 \le f < f_1 \\ w\mathcal{L}(f, f_1, f_2) & f_1 \le f < f_3 \,, \end{cases} \qquad (13)$$

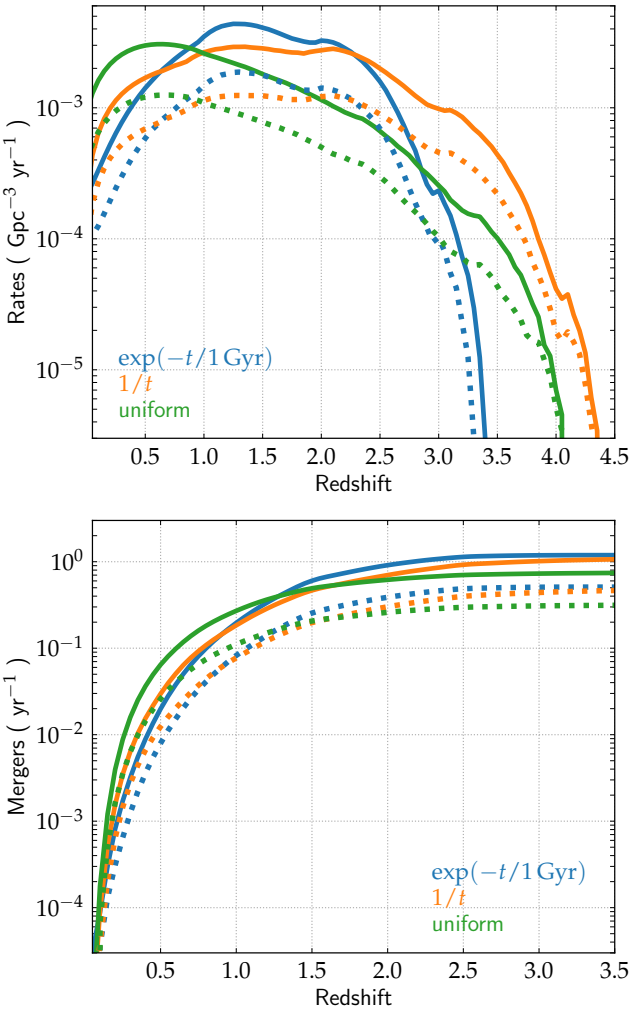


Figure 4. Comoving (top) and cumulative (bottom) merger rates for SMBH-IMBH binaries from cluster disruptions in galactic nuclei ($f_{\rm GC}^{\rm IMBH} = 1.0$ and $\zeta = 0.001$). Different colors represent different assumptions on delay times from cluster disruptions to SMBH-IMBH mergers. Solid lines: $M_{\rm GC,min} = 10^5\ M_\odot$; dotted lines: $M_{\rm GC,min}$ from Eq. 11 for late-type galaxies.

where

$$f_k = \frac{a_k\eta^2 + b_k\eta + c_k}{\pi(GM_z/c^3)}, \tag{14}$$

$$\mathcal{L} = \left(\frac{1}{2\pi}\right)\frac{f_2}{(f-f_1)^2 + f_2^2/4}, \tag{15}$$

$$w = \frac{\pi f_2}{2}\left(\frac{f_0}{f_1}\right)^{2/3}, \tag{16}$$

with $\eta = M_{\rm SMBH}M_{\rm IMBH}/(M_{\rm SMBH}+M_{\rm IMBH})^2$, and the values of $\{f_k, a_k, b_k, c_k\}$ are reported in Table 2 in Robson et al. (2019). In Eq. 13, f_0 is the observed (detector frame) frequency, related to the binary orbital frequency by $f_0 = (1+z)^{-1}f_{\rm orb}$, $M_{\rm c,z}$ is the redshifted chirp mass, related to the rest-frame chirp mass

$$M_{\rm c} = \frac{M_{\rm SMBH}^{3/5}M_{\rm IMBH}^{3/5}}{(M_{\rm SMBH}+M_{\rm IMBH})^{1/5}} \tag{17}$$

by $M_{\rm c} = M_{\rm c,z}/(1+z)$, and

$$D_{\rm L} = (1+z)\frac{c}{H_0}\int_0^z \frac{d\zeta}{\sqrt{\Omega_{\rm M}(1+\zeta^3)+\Omega_\Lambda}} \tag{18}$$

is the luminosity distance, where z is the redshift, and c and H_0 are the velocity of light and Hubble constant. We set $\Omega_{\rm M} = 0.286$ and $\Omega_\Lambda = 0.714$ (Planck Collaboration 2016)), respectively. We compute the power spectral density of LISA as in Eq. 1 in Robson et al. (2019).

We show in Figure 5 the cumulative distribution function of the SNR in LISA for a cosmological population of SMBH-IMBH mergers from cluster disruptions in galactic nuclei for different assumptions on the IMBH mass. In these models, $f_{\rm GC}^{\rm IMBH} = 1.0$ and the delay time follows an exponential distribution with mean $\tau = 1\,$Gyr We find that about 90%, 80%, 50% of the binaries have SNR larger that 10, 30, 100, respectively, with a little dependence on ζ. This clearly shows that LISA can detect with good confidence the large majority of the SMBH-IMBH mergers predicted in our model.

4. DISCUSSION AND CONCLUSIONS

LISA offers a unique opportunity to discover IMBHs out to large redshifts and to make a big push forward in our understanding of their demographics. The implications of the possible existence of a large population of IMBHs in the Universe have only begun to be explored and only a handful of theoretical models that predict mass spectrum, redshift evolution, and merger rates of IMBH binaries have been developed.

We have built a semi-analytical framework to model cluster disruptions in galactic nuclei and formation of SMBH-IMBH binaries. We have shown that the comoving merger rate is $\sim 10^{-4}$ Gpc^{-3} yr^{-1} in the local Universe for a unity IMBH occupation fraction, scales linearly with it, and has a peak at $z \approx 0.5$-3, depending on the assumed distribution of delay times. Moreover, we have predicted ~ 0.1 event yr^{-1} within redshift $z \approx 3.5$ if 10% of star clusters host an IMBH, while ~ 1 yr^{-1} for a unity occupation fraction. More than 90% of these systems will be detectable with LISA with an SNR larger than 10, with half of them being detectable with an SNR larger than 100.

Our models represent an effective way, calibrated over the state-of-the-art results in the literature, to model the complex interplay between galaxy assembly, star cluster disruptions, and growth of the innermost regions of galaxies. Nevertheless, there are some limitations to our approach. In our models, we have assumed that the SMBH exists since the beginning of the NSC build-up. However, the mass of SMBHs evolves across cosmic

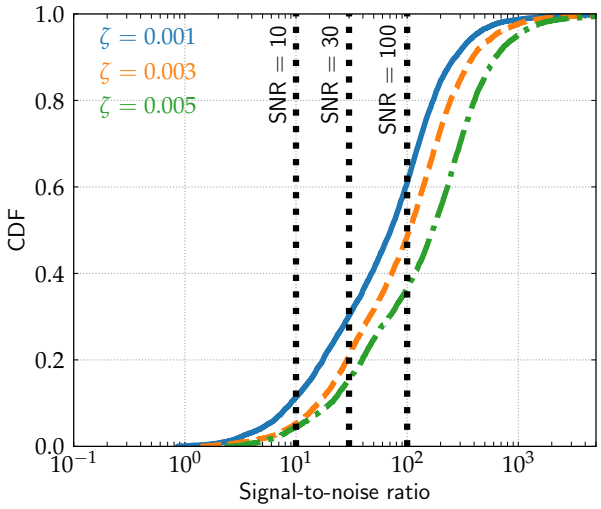


Figure 5. Cumulative distribution function of the SNR in LISA for a cosmological population of SMBH-IMBH mergers from cluster disruptions in galactic nuclei. Different colors represent different assumptions on the IMBH mass, assumed to be a fraction ζ of its parent cluster.

time probably starting from smaller seed BHs, with the exact seeding mechanism not known. These seed BHs could have originated either from the evolution of massive stars or they may have formed with large initial masses through direct collapse of gas, and could subsequently grow from gas accretion, disruption of stars, and mergers with other BHs (e.g., Volonteri 2010; Pacucci et al. 2015; Stone et al. 2017; Fragione & Silk 2020; Natarajan 2021; Askar et al. 2022). Smaller SMBH masses would affect the distribution of stars and compact remnants, ultimately impacting the disruption of inspiralling star clusters and IMBH dynamics in the innermost region of the galaxy. Since the strain of the GW signal depends on the chirp mass of the merging binary (see Eq. 12), smaller SMBH masses would also imply a smaller detectable volume for these type of events by LISA (Robson et al. 2019). Another caveat of our approach is the lack of a detailed prescription for the evolution of any formed SMBH-IMBH, which may depend on the specific orbit of the parent cluster, on the details of the local stellar density profile, on the number of IMBHs that are simultaneously delivered, and the possible presence of gas (e.g., Baumgardt et al. 2006; Portegies Zwart et al. 2006; Mastrobuono-Battisti et al. 2014; Dosopoulou & Antonini 2017). Finally, the mass distribution and the occupation fraction of IMBHs in dense star clusters is quite uncertain, which depend on the cluster initial density, primordial binary fraction, and the slope of the initial mass function (e.g., González et al. 2021; Weatherford et al. 2021). While the lack of confirmed IMBH detections in Galactic globular clusters seems to suggest a low occupation fraction (e.g., Greene et al. 2020), direct or indirect observations with next-generation observatories of the effect of IMBHs on the surrounding stars and compact objects will be crucial to constrain their numbers with high confidence (e.g., Gill et al. 2008; Leigh et al. 2014; Brightman et al. 2016; Pasquato et al. 2016; Anninos et al. 2018; Mezcua et al. 2018; Barrows et al. 2019; Weatherford et al. 2020; Ward et al. 2021). Despite the limitations of our framework, our model gives reasonable estimates of SMBH-IMBH mergers as a result of the inspiral of GCs, consistent with current order-of-magnitude estimates in the literature (Arca-Sedda & Gualandris 2018; Arca-Sedda & Capuzzo-Dolcetta 2019).

A clear analysis of the role of all the above limitations and uncertainties could be given only by running a large set of N-body simulations, which are computationally expensive and beyond what current codes can handle. However, we can try to estimate and constrain the role of each of our assumption through the upcoming detections of GWs. Our models could be used to put an upper limit to the IMBH occupation fraction from the number of detected sources. For example, if LISA does not detect any SMBH-IMBH merger associated with galactic nuclei, our results would constrain the IMBH occupation fraction to $f_{\rm GC}^{\rm IMBH} \lesssim 0.3$. With ever-enhanced sensitivity and with new detectors coming online, the characteristics of the IMBH family can be finally worked out. The forecast through the next decade includes tens or even hundreds of GW events, promising to shed light on the origin of this elusive population.

ACKNOWLEDGEMENTS

We thanks the anonymous referee for useful comments. G.F. acknowledges support from NASA Grant 80NSSC21K1722.

REFERENCES

Amaro-Seoane, P., Audley, H., Babak, S., Baker, J., & et al. 2017, arXiv e-prints, arXiv:1702.00786. https://arxiv.org/abs/1702.00786

Anninos, P., Fragile, P. C., Olivier, S. S., Hoffman, R., & et al. 2018, ApJ, 865, 3, doi: 10.3847/1538-4357/aadad9

Antonini, F. 2013, ApJ, 763, 62, doi: 10.1088/0004-637X/763/1/62

Antonini, F., Barausse, E., & Silk, J. 2015, ApJ, 812, 72, doi: 10.1088/0004-637X/812/1/72

Antonini, F., Capuzzo-Dolcetta, R., Mastrobuono-Battisti, A., & Merritt, D. 2012, ApJ, 750, 111, doi: 10.1088/0004-637X/750/2/111

Antonini, F., Gieles, M., & Gualandris, A. 2019, MNRAS, 486, 5008, doi: 10.1093/mnras/stz1149

Antonini, F., & Rasio, F. A. 2016, ApJ, 831, 187, doi: 10.3847/0004-637X/831/2/187
Arca Sedda, M., Berczik, P., Capuzzo-Dolcetta, R., Fragione, G., & et al. 2019, MNRAS, 484, 520, doi: 10.1093/mnras/sty3458
Arca-Sedda, M., & Capuzzo-Dolcetta, R. 2019, MNRAS, 483, 152, doi: 10.1093/mnras/sty3096
Arca-Sedda, M., & Gualandris, A. 2018, MNRAS, 477, 4423, doi: 10.1093/mnras/sty922
Askar, A., Davies, M. B., & Church, R. P. 2021, MNRAS, 502, 2682, doi: 10.1093/mnras/stab113
—. 2022, MNRAS, 511, 2631, doi: 10.1093/mnras/stab3741
Barrows, R. S., Mezcua, M., & Comerford, J. M. 2019, ApJ, 882, 181, doi: 10.3847/1538-4357/ab338a
Baumgardt, H., Gualandris, A., & Portegies Zwart, S. 2006, MNRAS, 372, 174, doi: 10.1111/j.1365-2966.2006.10818.x
Böker, T., van der Marel, R. P., Mazzuca, L., Rix, H.-W., & et al. 2001, AJ, 121, 1473, doi: 10.1086/319415
Brightman, M., Harrison, F. A., Barret, D., Davis, S. W., & et al. 2016, ApJ, 829, 28, doi: 10.3847/0004-637X/829/1/28
Capuzzo-Dolcetta, R., & Miocchi, P. 2008, MNRAS, 388, L69, doi: 10.1111/j.1745-3933.2008.00501.x
Capuzzo-Dolcetta, R., & Tosta e Melo, I. 2017, MNRAS, 472, 4013, doi: 10.1093/mnras/stx2246
Carson, D. J., Barth, A. J., Seth, A. C., den Brok, M., & et al. 2015, AJ, 149, 170, doi: 10.1088/0004-6256/149/5/170
Chandar, R., Whitmore, B. C., Kim, H., Kaleida, C., & et al. 2010, ApJ, 719, 966, doi: 10.1088/0004-637X/719/1/966
Di Carlo, U. N., Mapelli, M., Pasquato, M., Rastello, S., & et al. 2021, MNRAS, doi: 10.1093/mnras/stab2390
Dosopoulou, F., & Antonini, F. 2017, ApJ, 840, 31, doi: 10.3847/1538-4357/aa6b58
El-Badry, K., Quataert, E., Weisz, D. R., Choksi, N., & et al. 2019, MNRAS, 482, 4528, doi: 10.1093/mnras/sty3007
Fahrion, K., Leaman, R., Lyubenova, M., & van de Ven, G. 2021, arXiv e-prints, arXiv:2112.05610. https://arxiv.org/abs/2112.05610
Ferrarese, L., & Merritt, D. 2000, ApJL, 539, L9, doi: 10.1086/312838
Fragione, G., Ginsburg, I., & Kocsis, B. 2018a, ApJ, 856, 92, doi: 10.3847/1538-4357/aab368
Fragione, G., Kocsis, B., Rasio, F. A., & Silk, J. 2022, ApJ, 927, 231, doi: 10.3847/1538-4357/ac5026
Fragione, G., Leigh, N. W. C., Ginsburg, I., & Kocsis, B. 2018b, ApJ, 867, 119, doi: 10.3847/1538-4357/aae486
Fragione, G., & Silk, J. 2020, MNRAS, 498, 4591, doi: 10.1093/mnras/staa2629
Freitag, M., Gürkan, M. A., & Rasio, F. A. 2006, MNRAS, 368, 141, doi: 10.1111/j.1365-2966.2006.10096.x
Furlong, M., Bower, R. G., Theuns, T., Schaye, J., & et al. 2015, MNRAS, 450, 4486, doi: 10.1093/mnras/stv852
Georgiev, I. Y., Böker, T., Leigh, N., Lützgendorf, N., & Neumayer, N. 2016, MNRAS, 457, 2122, doi: 10.1093/mnras/stw093
Gieles, M. 2009, MNRAS, 394, 2113, doi: 10.1111/j.1365-2966.2009.14473.x
Giersz, M., Leigh, N. W., Hypki, A., Lützgendorf, N., & Askar, A. 2015, MNRAS, 454, 3150, doi: 10.1093/mnras/stv2162
Gill, M., Trenti, M., Miller, M. C., van der Marel, R., & et al. 2008, ApJ, 686, 303, doi: 10.1086/591269
Gnedin, O. Y., Ostriker, J. P., & Tremaine, S. 2014, ApJ, 785, 71, doi: 10.1088/0004-637X/785/1/71
González, E., Kremer, K., Chatterjee, S., Fragione, G., & et al. 2021, ApJL, 908, L29, doi: 10.3847/2041-8213/abdf5b
Gratton, R. G., Bragaglia, A., Carretta, E., Clementini, G., & et al. 2003, A&A, 408, 529, doi: 10.1051/0004-6361:20031003
Gratton, R. G., Fusi Pecci, F., Carretta, E., Clementini, G., & et al. 1997, ApJ, 491, 749, doi: 10.1086/304987
Greene, J. E., Strader, J., & Ho, L. C. 2020, ARA& A, 58, 257, doi: 10.1146/annurev-astro-032620-021835
Gürkan, M. A., Freitag, M., & Rasio, F. A. 2004, ApJ, 604, 632, doi: 10.1086/381968
Gürkan, M. A., & Rasio, F. A. 2005, ApJ, 628, 236, doi: 10.1086/430694
Jani, K., Shoemaker, D., & Cutler, C. 2020, Nature Astronomy, 4, 260, doi: 10.1038/s41550-019-0932-7
Kacharov, N., Neumayer, N., Seth, A. C., Cappellari, M., & et al. 2018, MNRAS, 480, 1973, doi: 10.1093/mnras/sty1985
Kormendy, J., & Ho, L. C. 2013, ARA& A, 51, 511, doi: 10.1146/annurev-astro-082708-101811
Kremer, K., Spera, M., Becker, D., Chatterjee, S., & et al. 2020, ApJ, 903, 45, doi: 10.3847/1538-4357/abb945
Larsen, S. S. 2009, A&A, 494, 539, doi: 10.1051/0004-6361:200811212
Leigh, N. W. C., Lützgendorf, N., Geller, A. M., Maccarone, T. J., & et al. 2014, MNRAS, 444, 29, doi: 10.1093/mnras/stu1437
Mapelli, M., Dall'Amico, M., Bouffanais, Y., Giacobbo, N., & et al. 2021, arXiv e-prints, arXiv:2103.05016. https://arxiv.org/abs/2103.05016

Mastrobuono-Battisti, A., Perets, H. B., & Loeb, A. 2014, ApJ, 796, 40, doi: 10.1088/0004-637X/796/1/40

Mezcua, M., Civano, F., Marchesi, S., Suh, H., & et al. 2018, MNRAS, 478, 2576, doi: 10.1093/mnras/sty1163

Miller, M. C., & Hamilton, D. P. 2002, MNRAS, 330, 232, doi: 10.1046/j.1365-8711.2002.05112.x

Minniti, D., Contreras Ramos, R., Zoccali, M., Rejkuba, M., & et al. 2016, ApJL, 830, L14, doi: 10.3847/2041-8205/830/1/L14

Natarajan, P. 2021, MNRAS, 501, 1413, doi: 10.1093/mnras/staa3724

Neumayer, N., Seth, A., & Böker, T. 2020, A& A Rev., 28, 4, doi: 10.1007/s00159-020-00125-0

O'Leary, R. M., Rasio, F. A., Fregeau, J. M., Ivanova, N., & O'Shaughnessy, R. 2006, ApJ, 637, 937, doi: 10.1086/498446

Pacucci, F., Volonteri, M., & Ferrara, A. 2015, MNRAS, 452, 1922, doi: 10.1093/mnras/stv1465

Pan, T., Loeb, A., & Kasen, D. 2012, MNRAS, 423, 2203, doi: 10.1111/j.1365-2966.2012.21030.x

Pasquato, M., Miocchi, P., Won, S. B., & Lee, Y.-W. 2016, ApJ, 823, 135, doi: 10.3847/0004-637X/823/2/135

Planck Collaboration. 2016, A&A, 594, A13, doi: 10.1051/0004-6361/201525830

Portegies Zwart, S. F., Baumgardt, H., McMillan, S. L. W., Makino, J., & et al. 2006, ApJ, 641, 319, doi: 10.1086/500361

Portegies Zwart, S. F., & McMillan, S. L. W. 2002, ApJ, 576, 899, doi: 10.1086/341798

Robson, T., Cornish, N. J., & Liu, C. 2019, Classical and Quantum Gravity, 36, 105011, doi: 10.1088/1361-6382/ab1101

Rossa, J., van der Marel, R. P., Böker, T., Gerssen, J., & et al. 2006, AJ, 132, 1074, doi: 10.1086/505968

Shen, S., Mo, H. J., White, S. D. M., et al. 2003, MNRAS, 978, 343, doi: 10.1046/j.1365-8711.2003.06740.x

Stone, N. C., Küpper, A. H. W., & Ostriker, J. P. 2017, MNRAS, 467, 4180, doi: 10.1093/mnras/stx097

Tagawa, H., Haiman, Z., & Kocsis, B. 2020, ApJ, 892, 36, doi: 10.3847/1538-4357/ab7922

Tremaine, S., Gebhardt, K., Bender, R., et al. 2002, ApJ, 574, 740, doi: 10.1086/341002

Tremaine, S. D., Ostriker, J. P., & Spitzer, L., J. 1975, ApJ, 196, 407, doi: 10.1086/153422

VandenBerg, D. A., Brogaard, K., Leaman, R., & Casagrande, L. 2013, ApJ, 775, 134, doi: 10.1088/0004-637X/775/2/134

Volonteri, M. 2010, A& A Rev., 18, 279, doi: 10.1007/s00159-010-0029-x

Ward, C., Gezari, S., Nugent, P., Bellm, E. C., & et al. 2021, arXiv e-prints, arXiv:2110.13098. https://arxiv.org/abs/2110.13098

Weatherford, N. C., Chatterjee, S., Kremer, K., & Rasio, F. A. 2020, ApJ, 898, 162, doi: 10.3847/1538-4357/ab9f98

Weatherford, N. C., Fragione, G., Kremer, K., Chatterjee, S., & et al. 2021, ApJL, 907, L25, doi: 10.3847/2041-8213/abd79c